Energy & Environmental Science

Cite this: *Energy Environ. Sci.*, 2012, **5**, 7931

www.rsc.org/ees

COMMUNICATION

Rechargeable Li–O_2 batteries with a covalently coupled $MnCo_2O_4$–graphene hybrid as an oxygen cathode catalyst†

Hailiang Wang,‡[a] Yuan Yang,‡[b] Yongye Liang,‡[a] Guangyuan Zheng,[c] Yanguang Li,[a] Yi Cui*[b] and Hongjie Dai*[a]

Received 26th March 2012, Accepted 23rd April 2012
DOI: 10.1039/c2ee21746e

We employ a $MnCo_2O_4$–graphene hybrid material as the cathode catalyst for Li–O_2 batteries with a non-aqueous electrolyte. The hybrid is synthesized by direct nucleation and growth of $MnCo_2O_4$ nanoparticles on reduced graphene oxide, which controls the morphology, size and distribution of the oxide nanoparticles and renders strong covalent coupling between the oxide nanoparticles and the electrically conducting graphene substrate. The inherited excellent catalytic activity of the hybrid leads to lower overpotentials and longer cycle lives of Li–O_2 cells than other catalysts including noble metals such as platinum. We also study the relationships between the charging–discharging performance of Li–O_2 cells and the oxygen reduction and oxygen evolution activity of catalysts in both aqueous and non-aqueous solutions.

Lithium ion batteries (LIBs) have become the main power source for today's portable electronics and are being actively pursued for propelling electric vehicles in the near future.[1–4] However, challenges remain for LIBs to become a major energy supply device for transportation. In particular, the energy density of LIBs should be increased by at least 3 times in order to support a driving range of more than 500 km with a single charge.[5] Also, the cost of LIBs should be lowered in order to be competitive with respect to other sources of energy. Limited by the insufficient capacity of electrode materials, the current LIB systems are not likely to reach the specific energy level needed for electric transportation in the long run.[1–5] It is necessary to develop alternative types of batteries that are capable of delivering higher energy density.

Li–O_2 batteries have recently attracted renewed interest due to significantly higher gravimetric energy density than LIBs.[5–7] With a theoretical specific energy of ~3500 W h kg^{-1} based on the mass of Li and O_2, Li–O_2 batteries are estimated to provide ~500 to 900 W h kg^{-1} in practical devices, which is more than 3 times higher than that of a typical LIB.[5–7] In an ideal Li–O_2 cell, a Li metal anode is oxidized while O_2 is reduced at the cathode during discharging, producing Li_2O_2 in an aprotic electrolyte or LiOH in an alkaline solution. During charging, Li_2O_2 or LiOH is supposed to be oxidized to generate O_2 at the cathode and Li is plated back onto the anode. Despite that numerous cathode catalysts including carbon, metal oxides and noble metals have been applied to enhance the sluggish kinetics of the oxygen reduction reaction (ORR) and oxygen evolution reaction (OER) at the cathode, Li–O_2 cells obtained thus far have exhibited high overpotential and short cycle lives.[5–12] It is important to understand the operating principles of Li–O_2 cells and to explore new oxygen electrode materials with higher catalytic

[a]*Department of Chemistry and Laboratory for Advanced Materials, Stanford University, Stanford, CA 94305, USA. E-mail: hdai@stanford.edu*
[b]*Department of Materials Science and Engineering, Stanford University, Stanford, CA 94305, USA. E-mail: yicui@stanford.edu*
[c]*Department of Chemical Engineering, Stanford University, Stanford, CA 94305, USA*

† Electronic supplementary information (ESI) available. See DOI: 10.1039/c2ee21746e

‡ These authors contributed equally to this work.

Broader context

A developing trend in the automobile industry now is to build electric vehicles that do not rely on fossil fuels and have zero emission. To provide electric vehicles with a driving range comparable to that of vehicles powered by gasoline or diesel, batteries with several times higher energy density than the existing Li ion batteries are needed. The Li–O_2 battery is such a choice. However, Li–O_2 cells obtained thus far have exhibited low round trip efficiency and short cycle lives mainly due to the sluggish kinetics of oxygen reduction and evolution reactions at the cathode. It is highly important to understand the scientific principles as well as to explore new oxygen electrode materials with higher catalytic activity for Li–O_2 cells. In this work, we design and fabricate Li–O_2 coin cells with a covalently coupled $MnCo_2O_4$–graphene hybrid material as a catalyst for the O_2 cathode. The cells show lower overpotentials and longer cycle lives than the ones catalyzed by other catalysts. We also study the relationships between the charging–discharging performance of Li–O_2 cells and the oxygen reduction/evolution activity of catalysts.

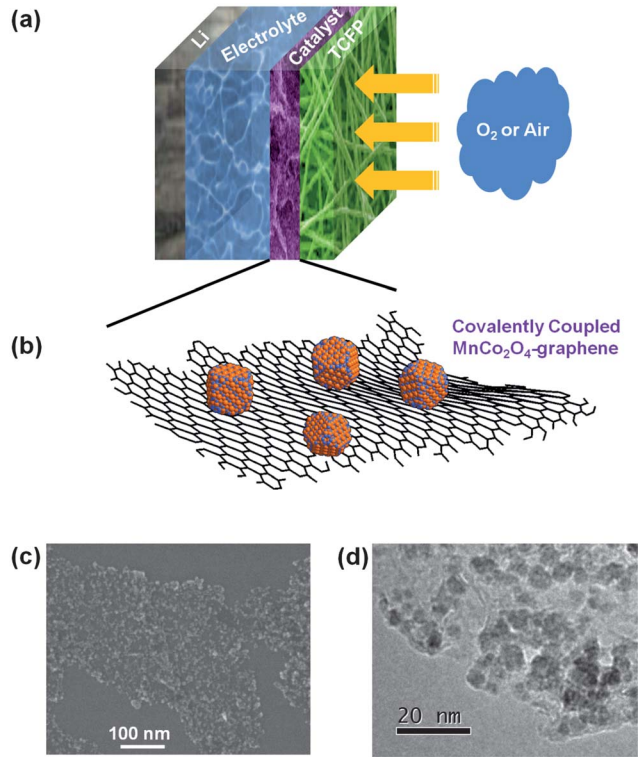

Fig. 1 $MnCo_2O_4$–graphene hybrid as a cathode catalyst for Li–O_2 batteries. (a) Schematic structure of the Li–O_2 cell catalyzed by the $MnCo_2O_4$–graphene hybrid. (b) Schematic structure of the $MnCo_2O_4$–graphene hybrid material comprised of $MnCo_2O_4$ nanoparticles covalently bonded to NGO sheets through carbon–oxygen–metal and carbon–nitrogen–metal bonds.[18] (c) An SEM image of the $MnCo_2O_4$–graphene hybrid. (d) A TEM image of the $MnCo_2O_4$–graphene hybrid.

activity to enhance the performance of Li–O_2 cells by lowering the overpotential and improving cycle life.

Transition metal oxides such as Co_3O_4 and MnO_2 have been reported to be catalytically active for Li–O_2 cells.[8,13–16] Recently, by growing Co_3O_4 nanoparticles on N doped mildly oxidized graphene sheets, we have synthesized a hybrid catalyst with excellent bi-functional activity for ORR and OER in aqueous alkaline solutions.[17] Through substitution of Mn^{3+} for Co^{3+} in the spinel lattice, ORR catalytic performance of the resulting Co(II)Co(III)Mn(III)O_4–graphene hybrid catalyst was further improved.[18] Covalent coupling between the oxide nanoparticles and graphene led to drastically improved catalytic activity of the hybrid over a physical mixture of the two by conventional means.[18] In this work we utilize the $MnCo_2O_4$–graphene hybrid material as a cathode catalyst for Li–O_2 cells (Fig. 1) and explore whether the ORR and OER electrocatalytic activities in aqueous solutions can be translated to organic electrolytes used for Li–O_2 batteries. At a current density of 100 mA g^{-1}, our Li–O_2 cell operating with a carbonate electrolyte exhibits a discharging voltage of ~2.95 V and a charging voltage of ~3.75 V, among the lowest overpotentials (similar to a Pt/C catalyst) reported in a similar electrolyte at comparable gravimetric current densities. The Li–O_2 cell with the $MnCo_2O_4$–graphene cathode catalyst also shows better charge–discharge cycling stability than that with a Pt/C catalyst. A capacity of 1000 mA h g^{-1} can be delivered for 40 cycles without significant increase in overpotential. The high cell performance is attributed to the excellent electrocatalytic activity of the $MnCo_2O_4$–graphene hybrid catalyst. The discharging performance of the Li–O_2 cell correlates well with the high ORR activity of our $MnCo_2O_4$–graphene hybrid catalyst in aqueous and non-aqueous solutions. However, we find that the OER catalytic activities of various catalysts in aqueous solutions do not correlate with the charging performance of relating Li–O_2 cells when comparing our hybrid catalyst with other materials including Pt/C.

The $MnCo_2O_4$–graphene hybrid was synthesized by a two step solution phase method in which $Co(OAc)_2$ and $Mn(OAc)_2$ were first hydrolyzed and coated onto graphene oxide (GO) in an ethanol–water mixed solvent with the addition of ammonium hydroxide. The suspension was then solvothermally treated to produce the hybrid material.[17,18] We showed recently that strong chemical coupling between Co_3O_4 nanoparticles with N doped reduced GO (NGO) substrates through covalent bonding led to excellent ORR and OER bi-functional catalytic activities in aqueous KOH solutions (Fig. 2a and b).[17] The $MnCo_2O_4$–graphene hybrid showed an enhanced ORR activity over the Co_3O_4–graphene hybrid due to an increase in the ORR active sites through Mn^{3+} substitution for Co^{3+} and an increase in the electrochemically active surface area.[18] The hybrid material showed much enhanced ORR and OER activities over free oxide nanoparticles physically mixed with conductive carbon (Fig. 2a and b).

We assessed the ORR catalytic activity of the $MnCo_2O_4$–graphene hybrid in a non-aqueous electrolyte of O_2-saturated 0.1 M $LiClO_4$ in propylene carbonate (PC) together with Pt/C, carbon black and a physical mixture of $MnCo_2O_4$ and NGO for comparison. Loaded onto Teflon coated carbon fiber papers (TCFPs), the catalysts exhibited a similar trend of relative activities as in aqueous media

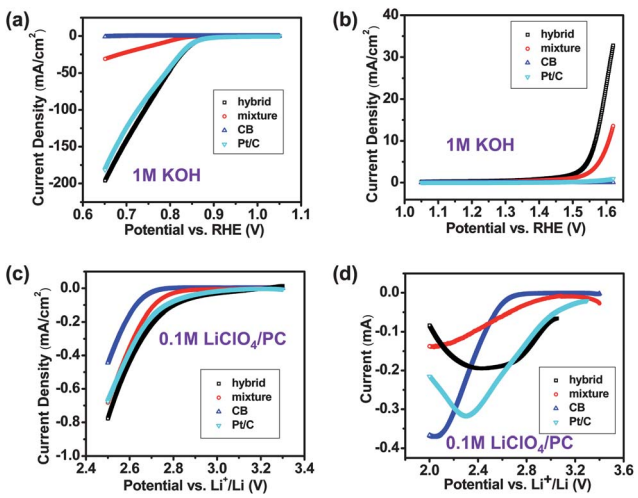

Fig. 2 ORR and OER with the $MnCo_2O_4$–graphene hybrid electrocatalyst in aqueous and non-aqueous media. (a) ORR catalytic activity of the hybrid compared to control catalysts in 1 M KOH solution. The mixture was made by physically mixing the free $MnCo_2O_4$ nanoparticles with NGO. CB stands for carbon black (Super P from Timcal). Pt/C is a commercial catalyst with 20 wt% Pt on Vulcan carbon black (from Fuel Cell Store). Catalysts were loaded on TCFP. (b) OER catalytic activity of the hybrid compared to control catalysts in 1 M KOH solution. Catalysts were loaded on TCFP. (c and d) ORR catalytic activity of the hybrid compared to control catalysts in 0.1 M $LiClO_4$/PC solution. Catalysts were loaded on TCFP (c) and glassy carbon electrode (d) respectively.

(Fig. 2a and c). At a potential of 2.8 V *vs.* Li^+/Li, the ORR current (corrected with current measured in an Ar-saturated electrolyte) of the hybrid electrode (~0.10 mA cm^{-2}) was slightly higher than that of the Pt/C electrode (~0.08 mA cm^{-2}), and much higher than those of the physical $MnCo_2O_4$ and NGO mixture (~0.03 mA cm^{-2}) and carbon black (~0.001 mA cm^{-2}). ORR measurements with catalysts loaded onto glassy carbon electrodes also confirmed the trend in relative activity of the catalysts (Fig. 2d). The $MnCo_2O_4$–graphene hybrid and Pt/C exhibited similar ORR onset potentials >3.0 V *vs.* Li^+/Li, considerably higher than those of the physical $MnCo_2O_4$ and NGO mixture (~3.0 V) and carbon black (~2.8 V). The electrochemical results suggested that our $MnCo_2O_4$–graphene hybrid could be an effective ORR catalyst for Li–O_2 batteries.

We made a Li–O_2 cell cathode by loading ~0.5 mg of the $MnCo_2O_4$–graphene hybrid material onto a ~1 cm^2 TCFP (Fig. S1a†). TCFP was widely used as a catalyst support and current collector in fuel cells.[17,18] We found it useful for preparing the oxygen electrode in Li–O_2 cells as the TCFP surface was not wetted by the electrolyte so that the gas could diffuse to the catalyst easily through the porous structure of TCFP. Our Li–O_2 cell was assembled with standard 2032 type coin cell cases except for the holes drilled in the positive side of the cases for oxygen intake (Fig. S1a and b†). Oxygen was prevented from reaching the anode by the electrolyte layer. It was a simple and efficient method to fabricate Li–O_2 cells utilizing commercial coin cell parts with minor modifications. 1 M $LiClO_4$ in PC was used as the electrolyte and Li metal served as the anode. The Li–O_2 cells were tested in a dry box with O_2 or air flow (Fig. S1c†).

Typical charge and discharge voltage profiles of our Li–O_2 cell are shown in Fig. 3a. At a current density of 100 mA g^{-1} based on the total mass of the $MnCo_2O_4$–graphene hybrid material, the average discharging voltage was about 2.95 V, close to the thermodynamic potential of the reaction $2Li^+ + 2e^- + O_2 \rightarrow Li_2O_2$, while the average charging voltage was about 3.75 V, ~0.8 V higher than the discharging voltage. This overpotential was comparable to that of precious metal based catalysts such as Pt/Au nanoparticles[9] and Pt/C,[19] and lower than those of other reported catalysts such as graphene,[10,20] metal oxides,[8,21] lithium metal oxides,[22] Pd–MnO_2,[14] MoN–graphene[11] and $CoMn_2O_4$–graphene,[16] at comparable current densities in similar carbonate electrolytes. The overpotential increased at higher current densities (Fig. 3a), but the charging potential at 400 mA g^{-1} was still below the high voltage limit of the electrolyte.[2,23] Cycle life of the Li–O_2 cell was tested with a capacity cut-off of 1000 mA h g^{-1} at a current density of 400 mA g^{-1}. The cell showed good cycling ability over 40 cycles in dry oxygen (Fig. 3c). During cycling, the final voltage of each discharging segment stabilized at ~2.5 to 2.6 V except for the first discharge, and the final voltage of each charging segment was in the range of ~4.2 to 4.3 V (Fig. 3b and d). This was among the best cycling performance of Li–O_2 cells operating in carbonate electrolytes.[8–16,20–22]

We further examined the discharge power rate of the Li–O_2 cell catalyzed by the $MnCo_2O_4$–graphene hybrid. Upon charging at a fixed current density of 200 mA g^{-1} for 15 h (Fig. 3f), the Li–O_2 cell was discharged to 2.0 V at various current densities (Fig. 3e). At 100 mA g^{-1}, a specific discharge capacity of ~3784 mA h g^{-1} was obtained based on the total mass of the $MnCo_2O_4$–graphene hybrid, which remained as ~2743 mA h g^{-1} at a high discharge current density of 800 mA g^{-1} (Fig. 3e), indicating high capacity and good rate capability of the cell.[8,11,13–16,20,21] This suggests that our $MnCo_2O_4$–graphene hybrid material holds promise in catalyzing Li–O_2 cells with high energy density.

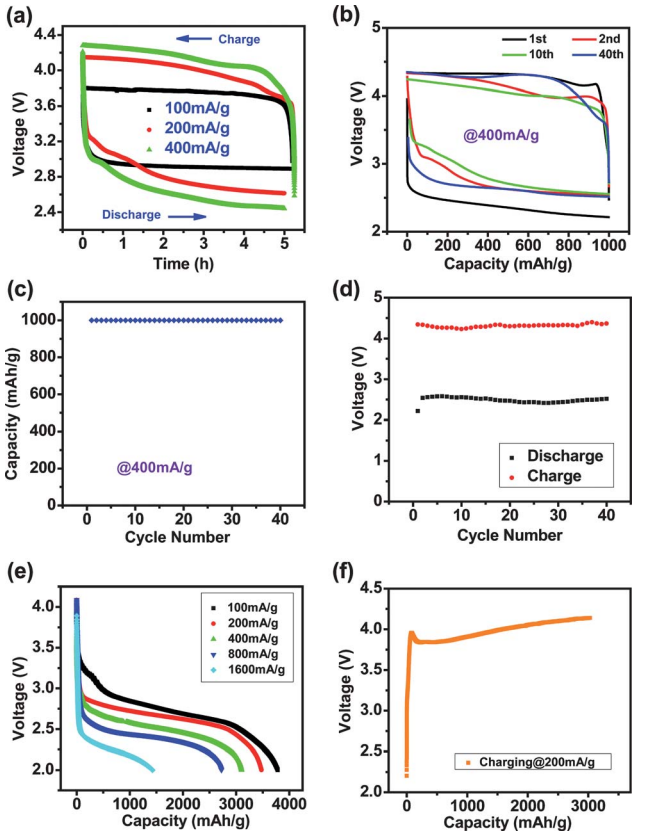

Fig. 3 A $MnCo_2O_4$–graphene hybrid catalyzed Li–O_2 cell. (a) Charging and discharging voltage profiles of the cell at various current densities. (b) Charging and discharging voltage profiles of the cell at various cycle numbers at a current density of 400 mA g^{-1}. (c) Specific discharge capacity of the cell over 40 cycles at 400 mA g^{-1}. (d) Cell voltage upon completion of each discharge (black) and charge (red) segment over the 40 cycles in (c). (e) Discharging voltage profiles of the cell at various current densities. (f) A typical charging voltage profile of the cell for power rate measurements in (e).

Since a practical Li–O_2 cell will utilize O_2 in ambient air instead of pure oxygen gas, we tested our Li–O_2 cells in dry air environment. A charge–discharge profile is plotted in Fig. S2a†. In dry air, the cell showed an average discharging voltage of ~2.85 V (Fig. S2a†), slightly lower than that in pure oxygen due to lower O_2 concentration in air. The average charging voltage was ~3.80 V, similar to that in pure oxygen. Our $MnCo_2O_4$–graphene catalyzed Li–O_2 cell also demonstrated good rechargeability in dry air. It was able to deliver a specific capacity of 1000 mA h g^{-1} for more than 20 cycles (Fig. S2b†).

In order to compare the catalytic properties of the $MnCo_2O_4$–graphene hybrid, we prepared Li–O_2 cells with other catalyst materials typically used in oxygen electrochemistry including N-doped graphene, metal oxide nanoparticles mixed with conducting carbon black, and Pt/C. The cells were discharged and charged at 100 mA g^{-1} with a capacity cut-off of 500 mA h g^{-1} and a high voltage cut-off of 4.5 V. Among these catalysts, carbon black showed the highest overpotential. Although discharging could be steadily performed at ~2.70 V (Fig. 4a, blue curve), the cell with carbon black as the cathode catalyst was barely rechargeable. The voltage reached the 4.5 V cut-off before the charging completed even at a low current

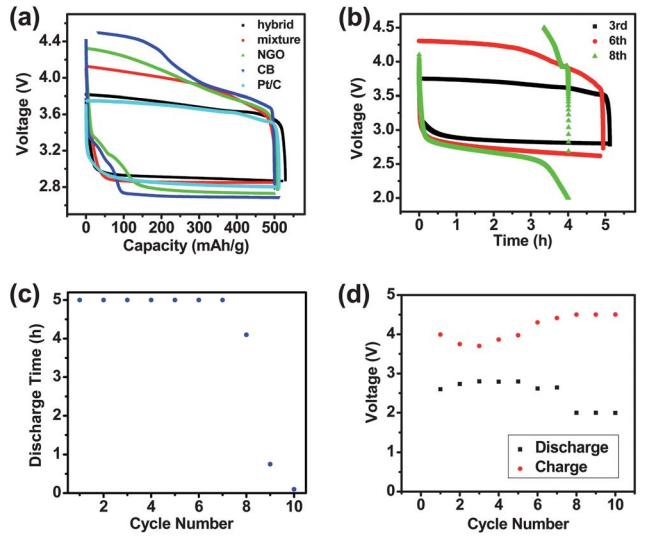

Fig. 4 Comparison of $MnCo_2O_4$–graphene hybrid material to other cathode catalysts in Li–O_2 cells. (a) Charging and discharging voltage profiles of Li–O_2 cells catalyzed by different catalysts at a current density of 100 mA g^{-1}. NGO was made in the same way as the $MnCo_2O_4$–graphene hybrid but without any metal precursors added (ref. 18 in text). (b) Charging and discharging voltage profiles of the Li–O_2 cell catalyzed by Pt/C at various cycle numbers. (c) Specific discharge capacity of the Li–O_2 cell catalyzed by Pt/C over 10 cycles. Current density was 100 mA g^{-1} for the first 6 cycles and 200 mA g^{-1} for the rest of cycles. (d) Cell voltage upon completion of each discharge (black) and charge (red) segment over the 10 cycles in (c).

density of 100 mA g^{-1} (Fig. 4a, green curve). NGO showed a slightly higher discharging voltage than carbon black as NGO with N doping was expected to be more active in ORR than non-doped carbon materials.[17,24] The charging voltage of the NGO catalyzed cell was lower than that of the carbon black cell. However the voltage still reached as high as 4.3 V at the end of the charging process, indicating poor catalytic activity of NGO for the charging reaction.

Physically mixing NGO with free $MnCo_2O_4$ nanoparticles reduced both the charging and discharging overpotentials considerably. At 100 mA g^{-1}, the Li–O_2 cell catalyzed by the mixture showed a discharging voltage of ~2.85 V and the charging completed at a voltage of ~4.10 V (Fig. 4a, red curve). However, the charging and discharging overpotentials of the mixture catalyzed Li–O_2 cell were still substantially higher than those of the cell catalyzed by the covalently coupled $MnCo_2O_4$–graphene hybrid (Fig. 4a, black curve).

We found that Pt/C was a similarly active catalyst to the $MnCo_2O_4$–graphene hybrid, significantly outperforming the free metal oxide nanoparticles mixed with conductive carbon (Fig. 4a, cyan curve). The high activity of Pt/C for Li–O_2 cells agrees with previous studies.[9,19] Despite relatively low overpotential in the initial cycles, the Pt/C catalyzed Li–O_2 cell showed a much faster increase in overpotential and shorter cycle life than the $MnCo_2O_4$–graphene hybrid catalyzed cell (Fig. 4b–d). The Pt/C cell was first cycled at 100 mA g^{-1} with a capacity cut-off of 500 mA h g^{-1} for 6 cycles. From the 3rd to the 6th cycle, the discharging voltage decreased to ~2.70 V from ~2.85 V, while the charging voltage increased to ~4.30 V from ~3.70 V (Fig. 4b and d). Current density was increased to 200 mA g^{-1} starting from the 7th cycle and a substantial decay in capacity was observed in the 8th cycle (Fig. 4b and c). The capacity of the Pt/C cell further dropped to zero in the 10th cycle (Fig. 4c). After 10 discharge–charge cycles, SEM imaging revealed that the Pt/C catalyst was buried in a thick layer of coating material (Fig. S3a and b†) likely resulted from side reactions. The coating appeared to be electrochemically inactive and was not removed during charging. In contrast, the $MnCo_2O_4$–graphene hybrid catalyst after 10 discharge–charge cycles retained its structure and morphology, without the formation of a thick coating layer (Fig. S3c and d†).

Although the NGO catalyzed Li–O_2 cell exhibited higher discharge voltage and lower charging voltage than the carbon black cell, there was still a substantially higher overpotential than that of the $MnCo_2O_4$–graphene hybrid cell, especially for the charging reaction. The voltage of the NGO cell was ~4.30 V upon completion of charging, ~0.50 V higher than that of the $MnCo_2O_4$–graphene hybrid cell. High recharging overpotential is often a problem associated with carbon material catalyzed Li–O_2 cells discussed in the literature, despite high specific capacity in the first discharge due to the large surface area of the carbon cathode.[10,12] Free $MnCo_2O_4$ nanoparticles physically mixed with NGO showed improved catalytic activity for Li–O_2 cells over NGO, comparable to other reported metal oxide nanocrystal catalysts mixed with conductive carbon.[8,21] Importantly, the lowest overpotential was achieved for the Li–O_2 cell catalyzed by the $MnCo_2O_4$–graphene hybrid, attributed to the excellent electrocatalytic activity afforded by the strong electrochemical coupling between the graphene sheets and the nanoparticles selectively grown and covalently bonded on graphene. Such intimate and effective interaction within the hybrid structure could result in fast and facile electron transfer through the conducting graphene network, which facilitates the charging and discharging reactions catalyzed on the surface of the oxide nanoparticles. Similar synergistic electrochemical effects have been also observed for various inorganic nanocrystals grown on reduced graphene oxide.[17,18,25–34] Although Pt/C was able to deliver as high catalytic activity as the $MnCo_2O_4$–graphene hybrid, the Pt/C catalyzed Li–O_2 cell was much less stable through charge–discharge cycling, caused by the formation of electrochemically inactive coating materials that could block the catalyst surface (Fig. S3†). Therefore the $MnCo_2O_4$–graphene hybrid could be a potential catalyst with high activity, good cycling stability and low cost for Li–O_2 batteries.

We found that the performances of various catalysts for the discharging reaction of the Li–O_2 cells (Fig. 4a) were consistent with the ORR activity trend measured in both non-aqueous (Fig. 2c and d) and aqueous electrolytes (Fig. 2a). However, the catalytic capability for the charging reaction in a non-aqueous electrolyte (Fig. 4a) was not directly correlated with the OER activity in aqueous solutions (Fig. 2b). In particular, Pt/C was barely active for OER in 1 M KOH solution, but was able to catalyze the charging reaction in Li–O_2 cells with low overpotential (similar to our hybrid which was differed from Pt/C with high OER activity in aqueous KOH solutions). This suggested that charging reactions in the Li–O_2 cells differed from OER and were not catalyzed by regular OER catalysts for aqueous systems. It has been recently reported that the discharge products of Li–O_2 cells with carbonate electrolytes are much more complicated than simple Li_2O_2.[35–37] A dominant amount of the solid discharge products could be comprised of lithium alkylcarbonates ($LiRCO_3$) and lithium carbonate (Li_2CO_3), resulted from nucleophilic attack on the organic carbonates by discharge intermediates such as superoxide ions (O_2^-) and the resulting decomposition of the carbonate electrolyte.[35–37] Although the carbonate electrolyte is frequently used in

the present Li–O_2 cells,[8–16,20–22] the issue of electrolyte degradation has to be solved before a stable Li–O_2 battery can be developed.[35–37] Moreover, we noticed that there was a significantly higher charging overpotential than that of discharging for all of the catalysts tested (Fig. 4a). The chemistry and catalysis involved in the charging process in Li–O_2 batteries are currently not understood. Such an understanding is needed in order to develop a new generation of catalysts with significantly improved activity for the charging reactions of Li–O_2 batteries.

In summary, we have shown a covalently coupled $MnCo_2O_4$–graphene hybrid material as an active, stable and low-cost cathode catalyst for Li–O_2 batteries. The Li–O_2 cell with the hybrid catalyst has similar low charge–discharge overpotentials as the Pt/C catalyzed cell, but with a much longer cycle life. Owing to electrochemical coupling between the graphene sheets and the $MnCo_2O_4$ nanoparticles in the hybrid, the material outperforms other metal oxide based and carbon based catalysts under similar measurement conditions, affording Li–O_2 coin cells with high capacity, low overpotential and good cycling stability. Further work is needed to understand and improve electrocatalysis in the charging reactions in Li–O_2 batteries.

Acknowledgements

This work is supported partially by Intel, a Stinehart Grant for Energy Research at Stanford from the Stanford Precourt Institute for Energy and a Stanford Graduate Fellowship.

References

1 M. Armand and J. M. Tarascon, *Nature*, 2008, **451**, 652–657.
2 J. B. Goodenough and Y. Kim, *Chem. Mater.*, 2010, **22**, 587–603.
3 B. Scrosati, J. Hassoun and Y.-K. Sun, *Energy Environ. Sci.*, 2011, **4**, 3287–3295.
4 V. Etacheri, R. Marom, R. Elazari, G. Salitra and D. Aurbach, *Energy Environ. Sci.*, 2011, **4**, 3243–3262.
5 P. G. Bruce, S. A. Freunberger, L. J. Hardwick and J. M. Tarascon, *Nat. Mater.*, 2012, **11**, 19–29.
6 G. Girishkumar, B. McCloskey, A. C. Luntz, S. Swanson and W. Wilcke, *J. Phys. Chem. Lett.*, 2010, **1**, 2193–2203.
7 J. S. Lee, S. T. Kim, R. Cao, N. S. Choi, M. Liu, K. T. Lee and J. Cho, *Adv. Energy Mater.*, 2011, **1**, 34–50.
8 A. Debart, J. Bao, G. Armstrong and P. G. Bruce, *J. Power Sources*, 2007, **174**, 1177–1182.
9 Y. C. Lu, Z. C. Xu, H. A. Gasteiger, S. Chen, K. Hamad-Schifferli and Y. Shao-Horn, *J. Am. Chem. Soc.*, 2010, **132**, 12170–12171.
10 Y. L. Li, J. J. Wang, X. F. Li, D. S. Geng, R. Y. Li and X. L. Sun, *Chem. Commun.*, 2011, **47**, 9438–9440.
11 S. M. Dong, X. Chen, K. J. Zhang, L. Gu, L. X. Zhang, X. H. Zhou, L. F. Li, Z. H. Liu, P. X. Han, H. X. Xu, J. H. Yao, C. J. Zhang, X. Y. Zhang, C. Q. Shang, G. L. Cui and L. Q. Chen, *Chem. Commun.*, 2011, **47**, 11291–11293.
12 Y. L. Li, J. J. Wang, X. F. Li, J. Liu, D. S. Geng, J. L. Yang, R. Y. Li and X. L. Sun, *Electrochem. Commun.*, 2011, **13**, 668–672.
13 G. Q. Zhang, J. P. Zheng, R. Liang, C. Zhang, B. Wang, M. Au, M. Hendrickson and E. J. Plichta, *J. Electrochem. Soc.*, 2011, **158**, A822–A827.
14 A. K. Thapa, Y. Hidaka, H. Hagiwara, S. Ida and T. Ishihara, *J. Electrochem. Soc.*, 2011, **158**, A1483–A1489.
15 A. K. Thapa, K. Saimen and T. Ishihara, *Electrochem. Solid-State Lett.*, 2010, **13**, A165–A167.
16 L. Wang, X. Zhao, Y. H. Lu, M. W. Xu, D. W. Zhang, R. S. Ruoff, K. J. Stevenson and J. B. Goodenough, *J. Electrochem. Soc.*, 2011, **158**, A1379–A1382.
17 Y. Y. Liang, Y. G. Li, H. L. Wang, J. G. Zhou, J. Wang, T. Regier and H. J. Dai, *Nat. Mater.*, 2011, **10**, 780–786.
18 Y. Liang, H. Wang, J. Zhou, Y. Li, J. Wang, T. Z. Regier and H. Dai, *J. Am. Chem. Soc.*, 2012, **134**, 3517–3523.
19 B. D. McCloskey, R. Scheffler, A. Speidel, D. S. Bethune, R. M. Shelby and A. C. Luntz, *J. Am. Chem. Soc.*, 2011, **133**, 18038–18041.
20 B. Sun, B. Wang, D. W. Su, L. D. Xiao, H. Ahn and G. X. Wang, *Carbon*, 2012, **50**, 727–733.
21 H. Cheng and K. Scott, *J. Power Sources*, 2010, **195**, 1370–1374.
22 L. Trahey, C. S. Johnson, J. T. Vaughey, S. H. Kang, L. J. Hardwick, S. A. Freunberger, P. G. Bruce and M. M. Thackeray, *Electrochem. Solid-State Lett.*, 2011, **14**, A64–A66.
23 K. Hayashi, Y. Nemoto, S. Tobishima and J. Yamaki, *Electrochim. Acta*, 1999, **44**, 2337–2344.
24 D. S. Geng, Y. Chen, Y. G. Chen, Y. L. Li, R. Y. Li, X. L. Sun, S. Y. Ye and S. Knights, *Energy Environ. Sci.*, 2011, **4**, 760–764.
25 H. L. Wang, H. S. Casalongue, Y. Y. Liang and H. J. Dai, *J. Am. Chem. Soc.*, 2010, **132**, 7472–7477.
26 H. L. Wang, Y. Yang, Y. Y. Liang, L. F. Cui, H. S. Casalongue, Y. G. Li, G. S. Hong, Y. Cui and H. J. Dai, *Angew. Chem., Int. Ed.*, 2011, **50**, 7364–7368.
27 H. L. Wang, Y. Y. Liang, Y. G. Li and H. J. Dai, *Angew. Chem., Int. Ed.*, 2011, **50**, 10969–10972.
28 Y. G. Li, H. L. Wang, L. M. Xie, Y. Y. Liang, G. S. Hong and H. J. Dai, *J. Am. Chem. Soc.*, 2011, **133**, 7296–7299.
29 H. L. Wang, L. F. Cui, Y. A. Yang, H. S. Casalongue, J. T. Robinson, Y. Y. Liang, Y. Cui and H. J. Dai, *J. Am. Chem. Soc.*, 2010, **132**, 13978–13980.
30 Y. Y. Liang, H. L. Wang, H. S. Casalongue, Z. Chen and H. J. Dai, *Nano Res.*, 2010, **3**, 701–705.
31 H. L. Wang, Y. Y. Liang, T. Mirfakhrai, Z. Chen, H. S. Casalongue and H. J. Dai, *Nano Res.*, 2011, **4**, 729–736.
32 J. Zhu, S. Chen, H. Zhou and X. Wang, *Nano Res.*, 2012, **5**, 11–19.
33 L. Yang, F. Xiaobin, Q. Junjie, J. Junyi, W. Shulan, Z. Guoliang and Z. Fengbao, *Nano Res.*, 2010, **3**, 429–437.
34 Z. Wang, H. Zhang, N. Li, Z. Shi, Z. Gu and G. Cao, *Nano Res.*, 2010, **3**, 748–756.
35 S. A. Freunberger, Y. H. Chen, Z. Q. Peng, J. M. Griffin, L. J. Hardwick, F. Barde, P. Novak and P. G. Bruce, *J. Am. Chem. Soc.*, 2011, **133**, 8040–8047.
36 W. Xu, K. Xu, V. V. Viswanathan, S. A. Towne, J. S. Hardy, J. Xiao, D. H. Hu, D. Y. Wang and J. G. Zhang, *J. Power Sources*, 2011, **196**, 9631–9639.
37 J. Xiao, J. Z. Hu, D. Y. Wang, D. H. Hu, W. Xu, G. L. Graff, Z. M. Nie, J. Liu and J. G. Zhang, *J. Power Sources*, 2011, **196**, 5674–5678.